Available online at www.sciencedirect.com
SCIENCE DIRECT®
Biomaterials 26 (2005) 6143–6150
Biomaterials
www.elsevier.com/locate/biomaterials

Plasma-treated nanostructured TiO_2 surface supporting biomimetic growth of apatite

Xuanyong Liu[a,b], Xiaobing Zhao[a,b], Ricky K.Y. Fu[b], Joan P.Y. Ho[b], Chuanxian Ding[a], Paul K. Chu[b,*]

[a]*Shanghai Institute of Ceramics, Chinese Academy of Sciences, 1295 Dingxi Road, Shanghai 200050, China*
[b]*Department of Physics & Materials Science, City University of Hong Kong, Kowloon, Hong Kong*

Received 27 January 2005; accepted 4 April 2005
Available online 31 May 2005

Abstract

Although some types of TiO_2 powders and gel-derived films can exhibit bioactivity, plasma-sprayed TiO_2 coatings are always bioinert, thereby hampering wider applications in bone implants. We have successfully produced a bioactive nanostructured TiO_2 surface with grain size smaller than 50 nm using nanoparticle plasma spraying followed by hydrogen plasma immersion ion implantation (PIII). The hydrogen PIII nano-TiO_2 coating can induce bone-like apatite formation on its surface after immersion in a simulated body fluid. In contrast, apatite cannot form on either the as-sprayed TiO_2 surfaces (both <50 nm grain size and >50 nm grain size) or hydrogen-implanted TiO_2 with grain size larger than 50 nm. Hence, both a hydrogenated surface that gives rise to negatively charged functional groups on the surface and small grain size (<50 nm) that enhances surface adsorption are crucial to the growth of apatite. Introduction of surface bioactivity to plasma-sprayed TiO_2 coatings, which are generally recognized to have excellent biocompatibility and corrosion resistance as well as high bonding to titanium alloys, makes them more superior than many current biomedical coatings.

Keywords: Nanostructured TiO_2; Bioactivity; Plasma spraying; Apatite; Hydrogen; Plasma immersion ion implantation

1. Introduction

Surfaces play an important role in the response of the biological environment to artificial medical devices such as implants. The physical, chemical and biochemical properties of the implant surface control performance-relevant processes such as protein adsorption, cell-surface interaction, and cell/tissue development at the interface between the body and the biomaterials. Nano-sized surface topography may give biomedical implants special and favorable properties in a biological environment. Webster et al. [1–3] revealed that nanophase ceramics could promote osseointegration that is critical to the clinical success of orthopedic/dental implants. Osteoblast proliferation was observed to be significantly higher on nanophase alumina, titania, and hydroxyapatite (HA) in comparison to their conventional counterparts. Furthermore, compared to conventional ceramics, synthesis of alkaline phosphatase and deposition of calcium-containing minerals were significantly enhanced on osteoblasts cultured on nanophase ceramics. We report here our success in producing a nanostructured, bioactive TiO_2 surface using a combination of nanoparticle plasma spraying and hydrogen plasma immersion ion implantation (PIII).

Compared to conventional coating techniques including the sol–gel method, plasma spraying is a more cost-effective and flexible means to deposit coatings with thicknesses ranging from micrometers to millimeters and it can be performed on large medical components

*Corresponding author. Tel.: +852 27887724; fax: +852 27887830.
E-mail addresses: xyliu@mail.sic.ac.cn (X. Liu), paul.chu@cityu.edu.hk (P.K. Chu).

0142-9612/$ - see front matter © 2005 Elsevier Ltd. All rights reserved.
doi:10.1016/j.biomaterials.2005.04.035

possessing a complicated shape such as hip joints. A plasma-sprayed bioceramic coating, such as HA, can improve the biological (bone conductivity and biocompatibility) properties of artificial implants made of titanium or titanium alloys. However, clinical use of plasma-sprayed HA coatings is plagued by their low crystallinity and poor bonding strength to titanium alloys. The low crystallinity gives rise to fast dissolution of the HA coating in contact with human body fluids subsequently shortening its lifetime [4], whereas the poor bonding strength results in delamination causing safety concerns [5].

Plasma-sprayed TiO_2 as bonding or composite coatings on Ti alloys has recently shown promising in vivo corrosion behavior as it acts as a chemical barrier against release of metal ions from the implants [6,7] in addition to its excellent biocompatibility [8]. Using UV illumination, Kasuga et al. [9] demonstrated the formation of apatite on compacted TiO_2 powders in simulated body fluids (SBF). The bioactivity of TiO_2 microspheres and sol–gel-derived titania films have also been investigated [10–12], but the bioactivity of plasma-sprayed TiO_2 is relatively unexplored. In fact, in our previous experiments [13], we could not observe apatite formation on as-sprayed TiO_2 coatings. Here, we report our new findings on the formation of a bioactive TiO_2 surface produced by nanoparticle plasma spraying and hydrogen PIII.

2. Materials and methods

Commercially available nano-sized TiO_2 powders (P25, Degussa, Germany) and submicro-sized TiO_2 powders (Wuhan Institute of Materials Protection, China) were made into sphere-like particles of 45–90 μm. The two types of particles were deposited onto Ti–6Al–4V substrates (10 mm × 10 mm × 2 mm) using an atmospheric plasma spraying (APS) system (Sulzer Metco, Switzerland) under the modified spray parameters. Argon (40 slpm (standard liter per minute)) and hydrogen (12 slpm) were used as primary and auxiliary arc gases, respectively. The feeding rate of powders was about 10 g/min using argon (3.5 slpm) as carrying gas. The arc current and voltage were 600 A and 70 V, respectively. The spraying distance was 100 mm. Coatings thickness for all specimens was about 100 μm. The surface and cross-sectional structures of the outermost layers of the as-sprayed TiO_2 coating produced from the nanoparticles were assessed using cold field-emission scanning electron microscopy (SEM) using a JEOL JSM-6700F and transmission electron microscopy (TEM) using a JEM2100F, respectively. Thin samples were prepared to allow TEM examination of the coating. Two coatings were first attached along their surfaces and then cut into a 1 mm thick specimen. The specimen was then attached to a tripod polisher with glue and polished from both sides until the thickness of the coating became about 30 μm. Finally, the thickness of the specimen was further reduced by employing a low-angle ion-thinning Precise Ion Polishing System (PIPS).

The micro-Raman spectra were acquired in the backscattering mode using a DILORyISA LabRAM 010 system equipped with an unpolarized HeNe laser. The excitation line wavelength was 632.8 nm and the laser power was 6.4 mW. The surface roughness of the as-sprayed TiO_2 coatings was determined using profilometry (HOMMELWERKE T-8000, Germany). The value reported here represents an average of five data points.

Hydrogen was implanted into the as-sprayed TiO_2 coating using a multifunctional plasma immersion ion implanter [14–16]. The plasma chamber was evacuated to a background pressure of 0.6 μTorr and then high-purity hydrogen gas was bled into the vacuum chamber to establish a working pressure of 0.5 mTorr. The instrumental parameters were as follows: pulse voltage 30 kV, pulse frequency 200 Hz, pulse duration 30 μs, RF discharge power 1000 W, and implantation time 2 h. After being ultrasonically washed in acetone and rinsed in deionized water, the as-sprayed and hydrogen-implanted TiO_2 coatings were soaked in SBF for 2 and 4 weeks at 36.5 °C without stirring to investigate their bioactivity. The samples were immersed in 40 ml SBF solution which was renewed every 7 days. The experiments were repeated three times for better statistics. The SBF solution was buffered at pH 7.4 with trimethanol aminomethane-HCl. The ionic concentrations in the solution are nearly equal to those in human body blood plasma [17]. The surface and cross-sections of the

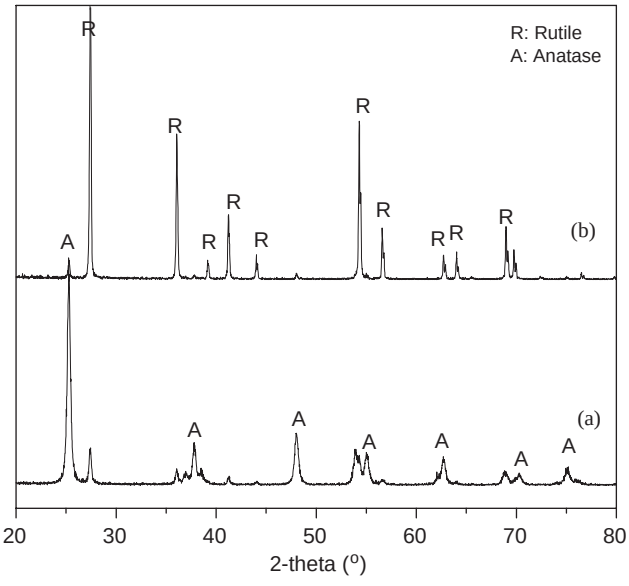

Fig. 1. XRD patterns of the original TiO_2 powders: (a) nano-sized and (b) submicro-sized.

coating after SBF immersion were observed using SEM. Energy-dispersive X-ray (EDS) analysis of the cross-section was conducted using an electron probe X-ray microanalysis system (EPMA-8705QH$_2$). The phase characterization of apatite-formed coating was conducted by X-ray diffraction (XRD) employing a diffractometer of JAPAN-RICOH with Ni-filtered Cu–Kα radiation ($\lambda = 1.5418$A). In the X-ray diffraction experiment the glancing angle of the incident beam against the surface of the specimen was fixed at 2°. A few micrograms of the Ca–P layer formed on the coating in SBF were scraped off. This was mixed with KBr and pressed into plates for structural analysis using Fourier transform infrared (FTIR) spectroscopy on a Bio Rad FTS-185.

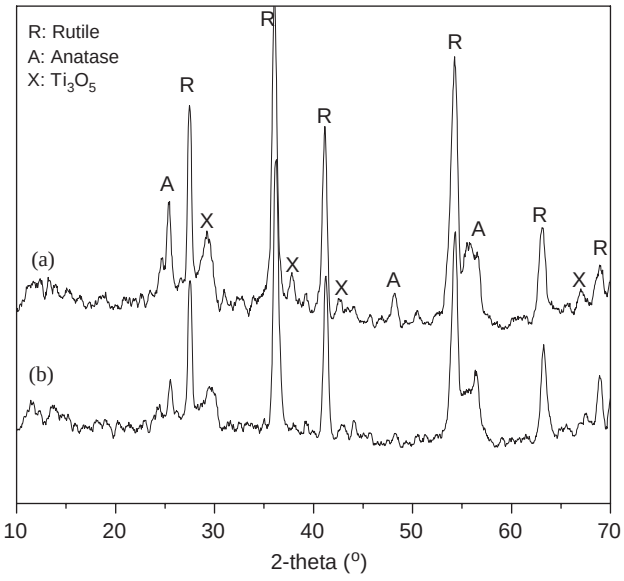

Fig. 2. XRD patterns of the as-sprayed TiO_2 surfaces: (a) nano-TiO_2 coating and (b) micro-TiO_2 coating.

3. Results and discussions

The XRD patterns of the two original powders indicate that the primary phase of the nano-sized powder is anatase (about 80%), while that of the submicro-sized powder is rutile (about 95%), as shown in Fig. 1.

The XRD patterns of the as-sprayed TiO_2 coatings synthesized with the two types of powders presented in Fig. 2 show that both coatings have primarily the rutile structure with a small amount of anatase and TiO_{2-x} suboxide (most of it is Ti_3O_5). The contents of anatase and suboxide in the coating obtained from the nano-sized TiO_2 particles (referred to as nano-TiO_2 coating) are nearly equal to or slightly higher than those in the

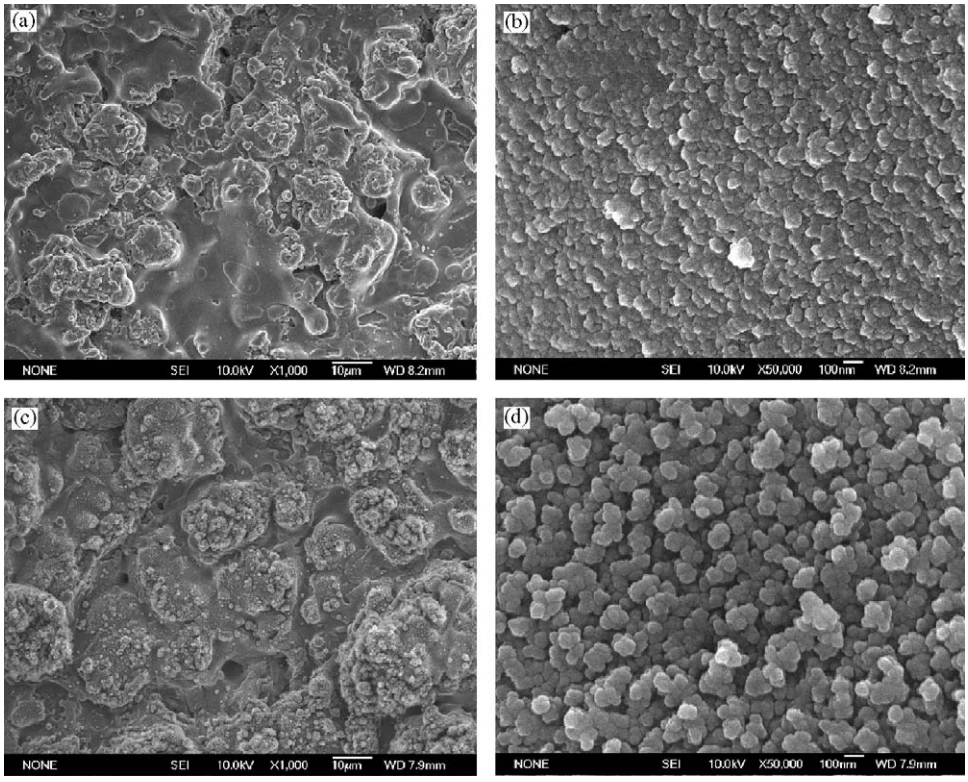

Fig. 3. Surface SEM views of as-sprayed TiO_2 surfaces: (a) nano-TiO_2 coating, (b) higher magnification of (a), (c) micro-TiO_2 coating, and (d) higher magnification of (c).

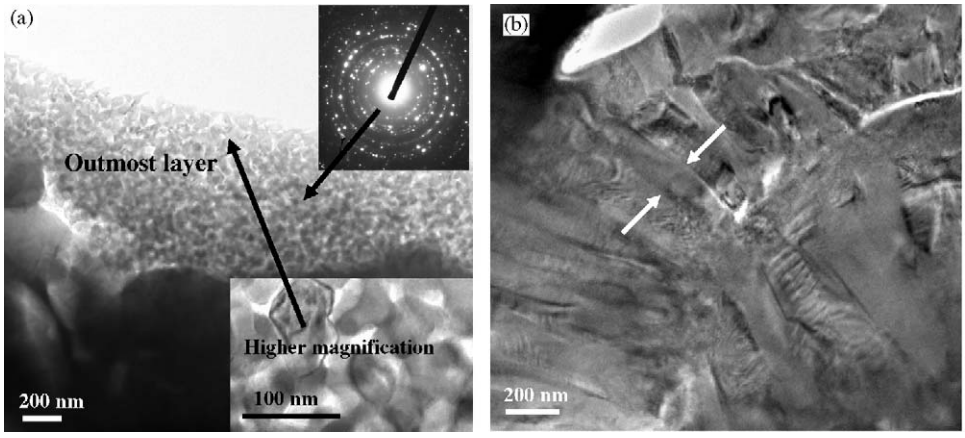

Fig. 4. Cross-sectional TEM views of the as-sprayed nano-TiO_2 coating: (a) coating surface and (b) coating interior.

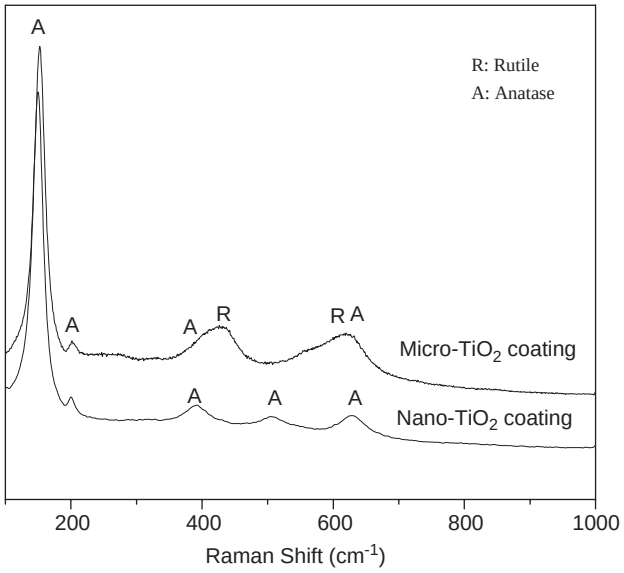

Fig. 5. Raman spectra obtained from the as-sprayed nano- and micro-TiO_2 coatings.

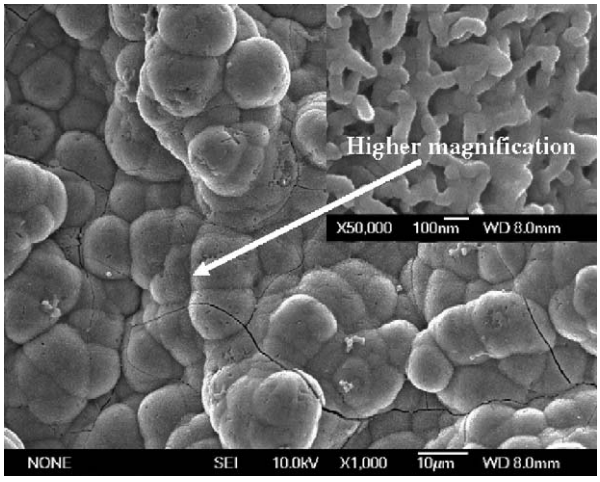

Fig. 6. Surface SEM views of the hydrogen PIII nano-TiO_2 coating after soaking in SBF for 2 weeks.

coating obtained from the submicro-sized TiO_2 powders (referred to as micro-TiO_2 coating). Although the anatase and rutile contents in the submicro-sized and nano-sized TiO_2 powders are different, the molten TiO_2 tends to be rutile and retains a partial anatase structure because plasma spraying is a rapid heating/cooling solidification process. The deoxidization of TiO_2 is due to the cooling rate of the molten or partially molten droplets in excess of 10^6 K/s and low oxygen partial pressure during plasma spraying.

The surface views of the as-sprayed TiO_2 coatings are displayed in Fig. 3. The nano-TiO_2 coating shows a relatively smoother surface. The average roughnesses of the as-sprayed nano- and micro-TiO_2 coatings are 8.20 and 10.97 μm, respectively. Many protuberances exist on the surface of the micro-TiO_2 coating (Fig. 3c). It is because the nano-sized powders are more easily melted during plasma spraying. The high magnification views indicate that the surface of the nano-TiO_2 coating comprises particles less than 50 nm in size (Fig. 3b), whereas the surface of the micro-TiO_2 coating is made of particles larger than 50 nm (Fig. 3d). The cross-sectional TEM views of the as-sprayed nano-TiO_2 coating also reveal that the outermost surface is composed of grains less than 50 nm in size (Fig. 4a) and are consistent with the SEM results depicted in Fig. 3a. The thickness of this outer layer is about 500 nm. Unfortunately, these grains are too small to determine their phase composition (anatase or rutile) using selected electron diffraction (SAD). In the interior of the coating, most of the grains exhibit a columnar morphology with a diameter of about 100–200 nm, as shown in Fig. 4b. The difference in the crystal growth between the surface and interior of the coating depends mostly on the thermal history. During plasma spraying, the bulk of the coating tends to possess larger columnar grains due to the continuous heat provided by the

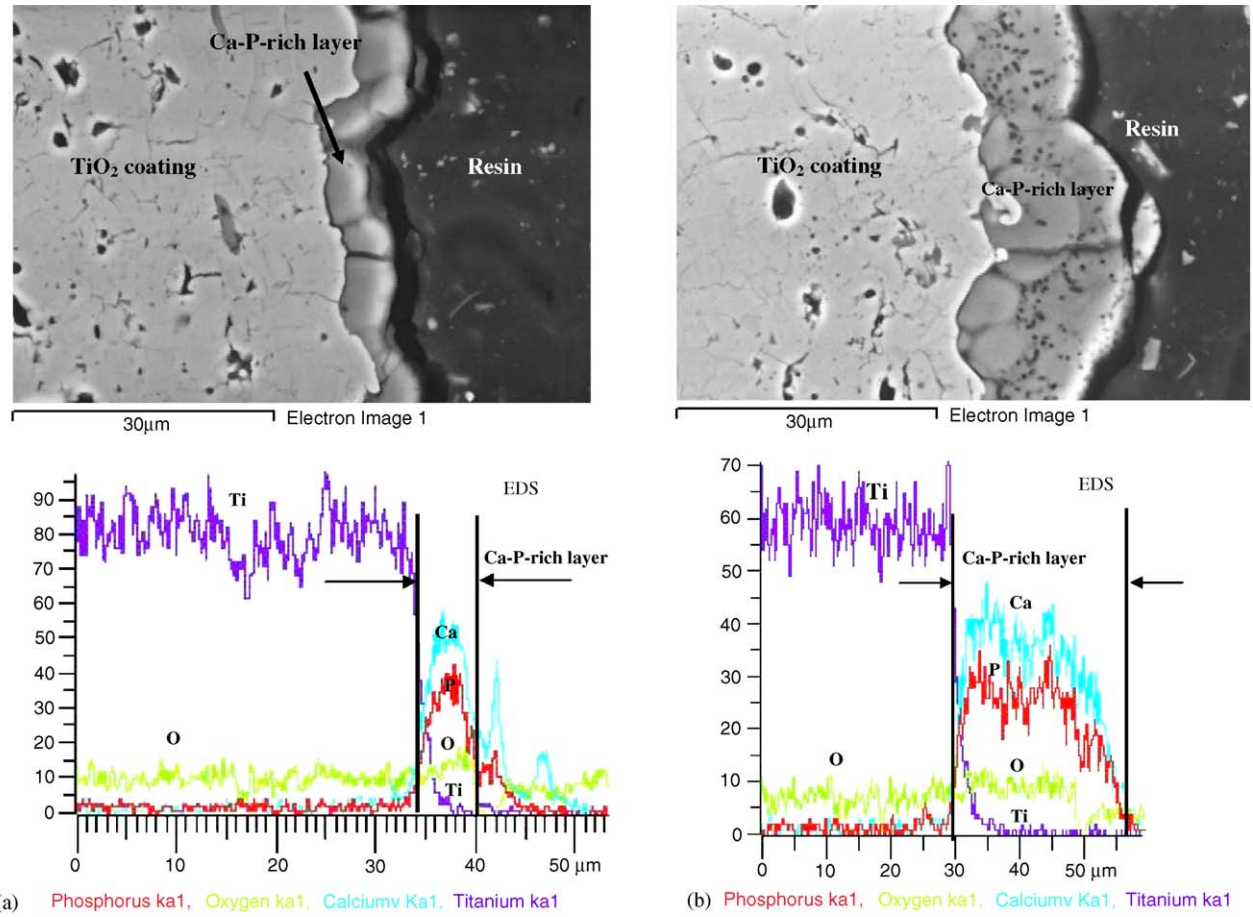

Fig. 7. Cross-sectional SEM views and EDS analysis of the hydrogen PIII nano-TiO_2 coating after soaking in SBF for (a) 2 weeks and (b) 4 weeks.

plasma and subsequent melt, whereas the surface grains are subjected to less heating.

The Raman spectra (100–1000 cm^{-1}) obtained from the as-sprayed nano- and micro-TiO_2 coatings are shown in Fig. 5. The peaks around 152, 200, 390, 510, and 630 cm^{-1} corresponding to nano-sized anatase are observed in both the as-sprayed nano- and micro-TiO_2 coatings. In addition, the broad peaks around 350–480 and 530–680 cm^{-1} observed for the micro-TiO_2 coating contain vibrational peaks around 440 and 610 cm^{-1} that correspond to anatase as well as peaks around 510 and 630 cm^{-1} corresponding to rutile. Therefore, the outermost layers of both the as-sprayed nano- and micro-TiO_2 coatings are primarily composed of nano-sized anatase, while a small quantity of rutile also exists in the as-sprayed micro-TiO_2 coating.

After immersion in SBF for two weeks, the surface of the hydrogen PIII nano-TiO_2 coating was completely covered by a newly formed layer, as shown in the surface views (Fig. 6). At a higher magnification, the newly formed layer exhibits a subtle net-like structure consisting of nano-sized rods. The cross-section views of the hydrogen PIII nano-TiO_2 coating soaked in SBF for two and four weeks show that the newly formed layer is Ca–P-rich with a thickness of about 5 μm after two weeks and about 25 μm after four weeks (Fig. 7). The XRD and FTIR results (Fig. 8) indicate that the new layer formed on the hydrogen PIII nano-TiO_2 coating consists of carbonate-containing HA. In contrast, in our control experiments involving the as-sprayed nano-TiO_2 and micro-TiO_2 coatings as well as the hydrogen PIII micro-TiO_2 coating and hydrogen PIII polished nano-TiO_2 coating from which the nanostructured surface is removed, no new precipitates can be observed on the surfaces after they are soaked in SBF for two weeks, as shown in Fig. 9.

Our results indicate that only the hydrogen PIII nano-TiO_2 coating with nanostructured surface possesses carbonate-containing HA formability. It can thus be inferred that the bioactivity of the plasma-sprayed TiO_2 coating depends on two factors: nanostructured surface composed of enough small particles and hydrogen incorporation. In fact, our other experiments also show that apatite can form on the surface of the nano-TiO_2 coating in SBF under UV illumination, while it cannot form on the surface of the micro-TiO_2 coating.

It has been suggested that OH groups on ceramic surfaces are effective in inducing the formation of a

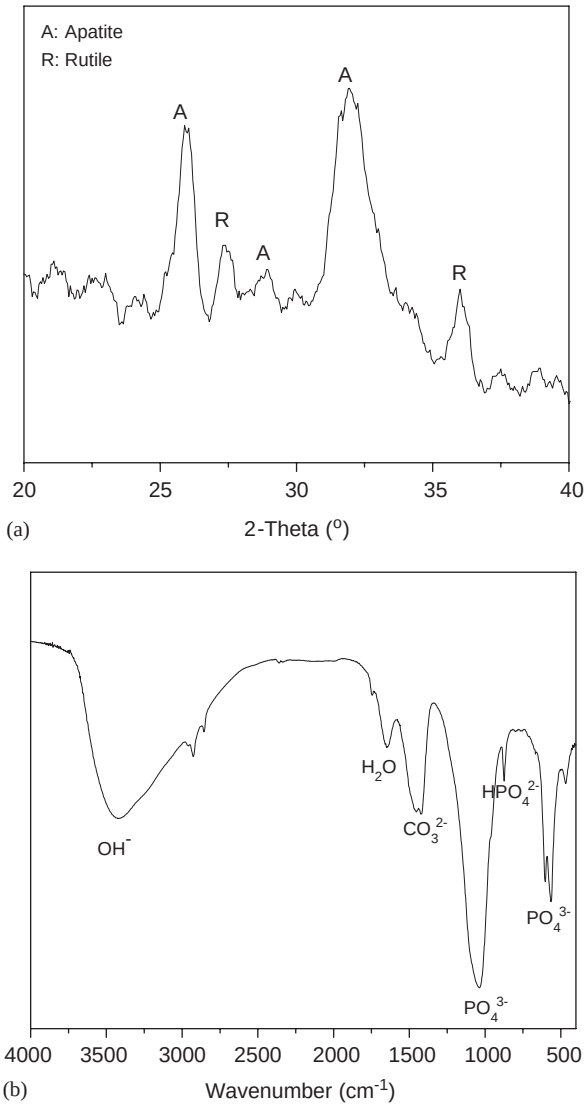

Fig. 8. Thin-film XRD patterns (a) and FTIR spectrum (b) of the hydrogen PIII nano-TiO_2 coating after soaking in SBF for 4 weeks.

carbonate-containing HA layer. For instance, gel-derived TiO_2 has been shown to induce surface carbonate-containing HA formation, but single-crystal anatase and titania synthesized by hydrothermal methods cannot [18]. The difference is believed to be due to the Ti–OH functional groups forming a negatively charged surface on the titania gel. We also believe this to be one of the reasons for the surface bioactivity of the hydrogen PIII nano-TiO_2 and the lack of it on the as-sprayed TiO_2 coatings.

The as-sprayed TiO_2 coating is highly oxygen deficient. While the outermost surface of the as-sprayed TiO_2 coating can be immediately reoxidized via oxygen adsorption after it is exposed to air [19], the subsurface region in the coating is still oxygen deficient. Therefore, suboxides such Ti_3O_5 can be detected by XRD. During hydrogen PIII, hydrogen ions react with the outermost bridge oxygen to form Ti–OH bonds because the reaction is energetically favorable, and two Ti(IV) are reduced to Ti(III) [20]. Eventually, a hydrogenated surface forms on the TiO_2. When the hydrogen PIII TiO_2 surface is soaked in SBF, Ti–OH reacts with the hydroxyl ion in the SBF to produce a negatively charged surface with the functional group $Ti–O^-$ as follows:

$$Ti-OH + OH^- \rightarrow Ti-O^- + H_2O.$$

Adsorption of ions and molecules on the solid surface is a critical step in crystal growth. The deposition of calcium ions is the first and most crucial step of carbonate-containing HA nucleation from an ionic solution. This process is believed to initiate the growth of bone-like apatite on the surface of biocompatible implants [21]. The formation of a negatively charged surface gives rise to apatite precipitation because positive calcium ions are attracted from the solution [18]. Our results show that in addition to hydrogen implantation that leads to a negatively charged surface, the formation of a nanostructured surface composed of enough small particles (<50 nm) is required for the formation of carbonate-containing HA. The dependence of the adsorption of molecules and ions on the particle size has been investigated. Vayssières et al. [22] have suggested that finer nanocrystalline particles have higher surface charge densities than larger ones. Zhang et al. [23] reported a 70-fold increase in the adsorption coefficient when a variety of organic acids were adsorbed onto 6 nm compared to 16 nm nanocrystalline titania particles. Peltola et al. [24] revealed that in gel-derived TiO_2 coatings, the outermost surface (nanometer scale) promoted apatite nucleation when the peak distance distribution was between 15 and 50 nm, and when the peak distance was greater than 50 nm, no significant in vitro bioactivity could be observed. The observed bioactivity of our hydrogen PIII nano-TiO_2 coating stems from a composite effect encompassing a negatively charged surface after hydrogen PIII as well as enhanced adsorption onto the nanostructured surface. It can be demonstrated by thermodynamic analysis that the surface or interfacial tension diminishes with decreasing particle size as a result of the increase in the potential energy of the bulk atoms of the particles [23]. Smaller particles with increased molar free energy are more likely to adsorb molecules or ions per unit area onto their surfaces in order to decrease the total free energy and to become more stable. The overall effect is a sufficiently high adsorption coefficient on the nano-TiO_2 surface so that carbonate-containing HA can form.

4. Conclusion

Plasma-sprayed TiO_2 coatings have been produced using nano- or submicro-particles. The surface of the

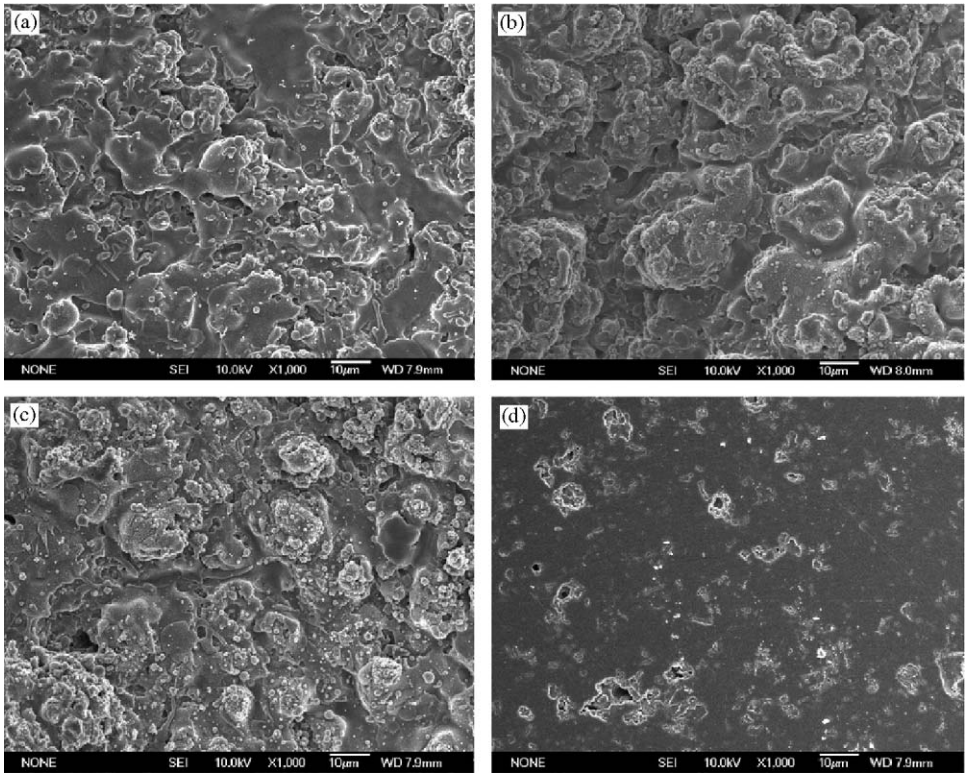

Fig. 9. Surface SEM views of various TiO_2 coatings soaked in SBF for 2 weeks: (a) as-sprayed nano-TiO_2 coating, (b) as-sprayed micro-TiO_2 coating, (c) hydrogen PIII micro-TiO_2 coating, and (d) hydrogen PIII polished nano-TiO_2 coating (the nanostructured surface is removed).

TiO_2 coating produced from the nanoparticles comprise particles less than 50 nm in size, whereas the surface of the TiO_2 coating produced from the submicro-particles is composed of particles larger than 50 nm. Both coatings have primarily the rutile structure with a small amount of anatase and TiO_{2-x} suboxide (most of it is Ti_3O_5). However, the phase compositions of their outermost layer are mostly anatase. After hydrogen PIII, the nano-TiO_2 coating exhibits excellent bioactivity. The hydrogen PIII nano-TiO_2 coating can induce carbonate-containing HA formation on its surface after immersion in an SBF. In contrast, carbonate-containing HA cannot form on either the as-sprayed TiO_2 surfaces (both <50 nm grain size and >50 nm grain size) or hydrogen-implanted TiO_2 with grain size larger than 50 nm. The bioactivity of the plasma-sprayed TiO_2 coating depends on a nanostructured surface composed of enough small particles in addition to hydrogen incorporation which yields the favorable surface functional groups for carbonate-containing HA formation.

Acknowledgments

This work was supported by Shanghai Science and Technology R&D Fund under grants 02QE14052 and 03JC14074, Innovation Fund of SICCAS under grant SCX200410, Hong Kong Research Grants Council (RGC) Competitive Earmarked Research Grants (CERG) CityU 1137/03E and Hong Kong Research Grants Council (RGC) Central Allocation Grant CityU 1/04C.

References

[1] Webster TJ, Siegel RW, Bizios R. Osteoblast adhesion on nanophase ceramics. Biomaterials 1999;20:1221–7.
[2] Webster TJ, Ergun C, Doremus RH, Siegel RW, Bizios R. Enhanced functions of osteoblasts on nanophase ceramics. Biomaterials 2000;21:1803–10.
[3] Webster TJ, Ergun C, Doremus RH, Siegel RW, Bizios R. Enhanced osteoclast-like cell functions on nanophase ceramics. Biomaterials 2001;22:1327–33.
[4] Fazan F, Marquis PM. Dissolution behavior of plasma-sprayed hydroxyapatite coatings. J Mater Sci: Mater Med 2000;1: 787–92.
[5] Lamy D, Pierrc AC, Heimann RB. Hydroxyapatite coatings with a bond coat of biomedical implants by plasma projection. J Mater Res 1996;11:680–6.
[6] Kurzweg H, Heimann RB, Troczynski T, Wayman ML. Development of plasma-sprayed bioceramic coatings with bond coats based on titania and zirconia. Biomaterials 1998;19: 1507–11.
[7] Nie X, Leyland A. Deposition of layered bioceramic hydroxyapatite/TiO_2 coatings on titanium alloys using a hybrid technique of micro-arc oxidation and electrophoresis. Surf Coat Technol 2000;125:407–14.

[8] Ratner BD. A perspective on titanium biocompatibility. In: Brunette DM, Tengvall P, Textor M, Thomsen P, editors. Titanium in Medicine. Berlin: Springer; 2001. p. 1–12.
[9] Kasuga T, Kondo H, Nogami M. Apatite formation on TiO_2 in simulated body fluid. J Cryst Growth 2002;23:5235–40.
[10] Keshmiri M, Troczynski T. Apatite formation on TiO_2 anatase microspheres. J Non-Cryst Solids 2003;324:289–94.
[11] Uchida M, Kim HM, Kokubo T, Fujibayashi S, Nakamura T. Structural dependence of apatite formation on titania gels in a simulated body fluid. J Biomed Mater Res 2003;64A:164–70.
[12] Peltola T, Pätsi M, Rahiala H, Kangasniemi I, Yli-Urpo A. Calcium phosphate induction by sol–gel-derived titania coatings on titanium substrates in vitro. J Biomed Mater Res 1998;41:504–10.
[13] Liu X, Ding C. Plasma sprayed wollastonite/TiO_2 composite coatings on titanium alloys. Biomaterials 2002;23:4065–77.
[14] Chu PK, Tang BY, Wang LP, Wang XF, Wang SY, Huang N. Third-generation lasma immersion ion implanter for biomedical materials and research. Rev Sci Instrum 2001;72:1660–5.
[15] Chu PK, Chen JY, Wang LP, Huang N. Plasma surface modification of biomaterials. Mater Sci Eng: Reports 2002;36:143–206.
[16] Chu PK. Recent developments and applications of plasma immersion ion implantation (PIII). J Vac Sci Technol B 2004;22:289–96.
[17] Kokubo T, Kushitani H, Sakka S, Kitsugi T, Yamamuro T. Solutions able to reproduce in vivo surface-structure changes in bioactive glass-ceramic A-W. J Biomed Mater Res 1990;24: 721–34.
[18] Li P, Ohtsuki C, Kokubo T, Nakanishi K, Soga N, De Groot K. The role of hydrated silica, titania, and alumina in inducing apatite on implants. J Biomed Mater Res 1994;28: 7–15.
[19] Pan JM, Maschhoff BL, Diebold U, Madey TE. Interaction of water, oxygen and hydrogen with TiO_2 (1 1 0) surfaces having different defect densities. J Vac Sci Technol A 1992;10: 2470–6.
[20] Leconte J, Markovits A, Skalli MK, Minot C, Belmajdoub A. Periodic ab initio study of the hydrogenated rutile TiO_2 (1 1 0) surface. Surf Sci 2002;497:194–204.
[21] Svetina M, Ciacchi LC, Sbaizero O, Meriani S, De Vita A. Deposition of calcium ions on rutile (1 1 0): a first-principles investigation. Acta Mater 2001;49:2169–77.
[22] Vayssières L, Chanéac C, Trone E, Joliver JP. Size Tailoring of magnetite particles formed by aqueous precipitation: an example of thermodynamic stability of nanometric oxide particles. J Colloid Interface Sci 1998;205:205–12.
[23] Zhang H, Penn RL, Hamers RJ, Banfield JF. Enhanced adsorption of molecules on surfaces of nanocrystalline particles. J Phys Chem B 1999;103:4656–62.
[24] Peltola T, Jokinen M, Rahiala H, Pätsi M, Heikkilä J, Kangasniemi I, Yli-Urpo A. Effect of aging time of sol on structure and in vitro calcium phosphate formation of sol-gel-derived titania films. J Biomed Mater Res 2000;51:200–8.